



City Research Online

City, University of London Institutional Repository

Citation: Mergos, P.E. ORCID: 0000-0003-3817-9520 and Mantoglou, F. (2020). Optimum design of reinforced concrete retaining walls with the flower pollination algorithm. *Structural and Multidisciplinary Optimization*, 61(2), pp. 575-585. doi: 10.1007/s00158-019-02380-x

This is the accepted version of the paper.

This version of the publication may differ from the final published version.

Permanent repository link: <https://openaccess.city.ac.uk/id/eprint/22619/>

Link to published version: <http://dx.doi.org/10.1007/s00158-019-02380-x>

Copyright and reuse: City Research Online aims to make research outputs of City, University of London available to a wider audience. Copyright and Moral Rights remain with the author(s) and/or copyright holders. URLs from City Research Online may be freely distributed and linked to.

City Research Online:

<http://openaccess.city.ac.uk/>

publications@city.ac.uk

Optimum design of reinforced concrete retaining walls with the flower pollination algorithm

Panagiotis E. Mergos^{a*}, Fotios Mantoglou^a

^a *Department of Civil Engineering, City, University of London, London, UK*

Abstract

The flower pollination algorithm (FPA) is an efficient metaheuristic optimization algorithm mimicking the pollination process of flowering species. In this study, FPA is applied, for first time, to the optimum design of reinforced concrete (RC) cantilever retaining walls. It is found that FPA offers important savings with respect to conventional design approaches and that it outperforms genetic algorithm (GA) and the particle swarm optimization (PSO) algorithm in this design problem. Furthermore, parameter tuning reveals that the best FPA performance is achieved for switch probability values ranging between 0.4 and 0.7, a population size of 20 individuals and a Lévy flight step size scale factor of 0.5. Finally, parametric optimum designs show that the optimum cost of RC retaining walls increases rapidly with the wall height and smoothly with the magnitude of surcharge loading.

Keywords: Optimization; flower pollination algorithm; reinforced concrete; retaining walls

1 Introduction

In many multimodal engineering design problems, conventional optimization techniques do not perform adequately as they are trapped in local optima. In these problems, the use of nature-inspired metaheuristic algorithms is recommended (Yang 2008). A great number of metaheuristic algorithms exist including genetic algorithms (GA) (Holland 1975), particle swarm optimization (PSO) (Kennedy 2011), firefly algorithm (FA) (Yang 2010), cuckoo search (CS) (Gandomi *et al.* 2013) and many others.

* Corresponding author. Panagiotis E. Mergos, Lecturer in Structural Engineering, Research Centre for Civil Engineering Structures, City, University of London, London, EC1V 0HB, UK.

E-mail address: panagiotis.mergos.1@city.ac.uk, Tel. 0044 (0) 207040 8417

Recently, Xin-She Yang (Yang 2012) developed the Flower Pollination Algorithm (FPA). FPA has been inspired by the evolution mechanism of flowering plants. It is a population-based metaheuristic algorithm recognised for its simplicity in formulation and efficiency in terms of computational performance (Alyasseri *et al.* 2018). As a result, FPA has been applied, with success, to numerous optimization problems in various scientific fields (Alyasseri *et al.* 2018). However, the number of applications of FPA to structural engineering problems is still rather limited. Bekdas *et al.* (2015) examined optimum structural design of steel truss structures using FPA and they found that it is directly competitive to other well-established optimization algorithms. Furthermore, Nigdeli *et al.* (2016) applied FPA to benchmark structural design problems related to plane frames, cantilever beams, I-beams and tubular columns and they found that FPA can be more robust and efficient than other algorithms. Moreover, Nigdeli *et al.* (2017) used a hybrid FPA version to obtain the optimal values of tuned mass dampers in frames subjected to earthquake excitations.

Reinforced concrete retaining walls are structures that are designed to resist lateral soil pressure in cases where there is a change in ground elevation. They are widely used in road construction and they typically involve large material volumes. Therefore, optimization of their design is essential. However, the significant number of independent design variables and the highly nonlinear constraints involved in the design of reinforced concrete structures (Mergos 2017, Mergos 2018) in general and the design of concrete retaining walls in particular make their optimum structural design a complex task that can only be performed efficiently by automated optimization algorithms.

A significant number of studies exist on the optimum design of RC cantilever retaining walls using different optimization algorithms. Saribas and Erbatur (1996) examined optimum design of earth-retaining walls using constrained nonlinear programming and assuming seven design variables determining geometry and steel reinforcement. Moreover, Ceranic *et al.* (2001) used simulated annealing (SA) algorithm to optimally design RC retaining walls employing seven independent design variables. Furthermore, Babu and Basha (2008) developed a reliability-based optimum design strategy of RC retaining walls that accounts for uncertainties in soil, steel and concrete mechanical properties. Yepes *et al.* (2008) performed an extensive parametric study on the optimum design of these walls structures using SA algorithm and assuming 20 independent design variables. Kaveh *et al.* (2010) investigated the optimum design of retaining walls employing the harmony search optimization algorithm. Khajehzadeh *et al.* (2010) applied a modified version of PSO with passive congregation to achieve economic design of RC retaining walls. Ghazavi *et al.* (2011) used the ant colony optimization technique

to minimize the cost of RC retaining walls. In a newer study, Yepes *et al.* (2012) extended their previous work on the optimum design of RC retaining walls to address not only minimum economic cost but also minimum embodied CO₂ emissions. It is recalled that concrete construction is one of the major contributors to global CO₂ emissions (Mergos 2018a, 2018b). Pei and Xia (2012) investigated the optimum design of retaining walls using different heuristic optimization algorithms such as GA, PSO and SA. Papazafeiropoulos *et al.* (2013) addressed the optimum seismic design of cantilever RC walls using numerical 2-D finite element simulations and genetic algorithms. Kaveh and Khayatazad (2014) developed optimal design solutions of cantilever retaining RC walls under earthquake loads by using the Ray optimization method. Furthermore, Khajehzadeh *et al.* (2014) examined multi-objective optimum design of retaining walls adopting a hybrid version of the adaptive gravitational search algorithm with pattern search setting economic cost and embodied CO₂ emissions as design objectives. Sheikholeslami *et al.* (2016) examined optimum design of these wall systems using a hybrid FA with upper bound strategy. Aydoglu (2017) examined the optimum seismic design of RC retaining walls using a biogeography-based optimization algorithm (BBO) with Lévy flights. Rahbari *et al.* (2017) investigated the optimum robust seismic design of retaining walls using GA and the response surface approach in combination with nonlinear dynamic finite element analyses. Gandomi *et al.* (2017) studied the optimum design of these wall systems using various evolutionary algorithms such as differential evolution (DE), evolutionary strategy (ES) and BBO.

The present study applies, for first time, the FPA algorithm to the structural design of RC cantilever retaining walls for minimum economic cost. The objective here is to examine the computational efficiency of FPA for this common structural design problem and compare it with other well-established optimization algorithms such as PSO and GA. Furthermore, an exploratory study is conducted to establish the FPA parameter values that maximize its performance in the design of these wall systems. Finally, a parametric study is conducted to show the effects of wall height and surcharge loading on the minimum costs of RC cantilever retaining walls.

2 Flower pollination algorithm

FPA mimics the evolution process of flowering plants via pollination. Flower pollination is either abiotic or biotic (Glover 2007, Yang 2012). Abiotic pollination occurs at short distances and it is therefore considered as a local pollination mechanism (Yang 2012). Biotic pollination

is facilitated by the pollinators (e.g. butterflies, bees and bats) that travel long distances. Therefore, it is treated as a global pollination procedure. The travel behaviour of pollinators can be well reproduced by Lévy flights (Pavlyukevich 2007). Another important characteristic of flower pollination is the so-called flower constancy. Indeed, pollinators tend to select specific flower species and neglect others (Yang 2012). In this way, pollinators reduce risks and ensure nectar intake. The afore-described features of flower pollination have been used to formulate the four basic rules of FPA algorithm:

1. Biotic pollination is treated as a global optimization process with pollinators conducting Lévy flights.
2. Abiotic pollination is treated as a local optimization procedure.
3. Flower constancy is taken into account by setting that the probability of reproduction is proportional to the level of similarity of the flowers involved.
4. The type of pollination procedure (local or global) is determined by a switch probability p that is a pre-fixed constant in $[0, 1]$.

In FPA, a candidate solution vector \mathbf{x}_i is represented by a flower i in a population of n flowers. To form the next population, the flowers perform either global or local pollination. The global pollination mechanism, in combination with the flower constancy rule, is modelled by the equation below:

$$\mathbf{x}_i^{t+1} = \mathbf{x}_i^t + \gamma \cdot L(\lambda) \cdot (\mathbf{g}^* - \mathbf{x}_i^t) \quad (1)$$

Where \mathbf{x}_i^t represents flower i at iteration t , \mathbf{g}^* is the best flower of all the population of flowers at iteration t , λ is a constant, γ is a constant scaling factor to control the step size, $L(\lambda) > 0$ is the Lévy flight step size that represents the strength of the pollination. A value of $\lambda = 3/2$ and $\gamma = 0.01$ is recommended by Yang (2012).

Furthermore, the local pollination mechanism, in combination with the flower constancy rule, is modelled by the following formula, where \mathbf{x}_j^t and \mathbf{x}_k^t are different flowers of the same population and ε is drawn from a uniform distribution in $[0, 1]$.

$$\mathbf{x}_i^{t+1} = \mathbf{x}_i^t + \varepsilon \cdot (\mathbf{x}_j^t - \mathbf{x}_k^t) \quad (2)$$

The fourth FPA rule determines the type of flower pollination (i.e. local or global). If a random number drawn in $[0, 1]$ is lower than p then global pollination is conducted. Otherwise, local

pollination is performed. A value of $p = 0.8$ is recommended in the original publication of FPA (Yang 2012). Taking the previous into consideration, Fig. 1 presents the pseudo-code of FPA.

```

Set objective  $\min f(\mathbf{x})$ ,  $\mathbf{x} = (x_1, x_2, \dots, x_d)$ 
Initialize a population of  $n$  flowers with random procedures
Determine the best solution  $\mathbf{g}^*$  of the initial population
Determine the value of switch probability  $p \in [0, 1]$ 
while ( $t < MaxIteration$ )
    for  $i = 1 : n$  (for all flowers of the population)
        if  $\text{rand} < p$ 
            Draw a  $d$ -dimensional Lévy distribution step vector  $L$ 
            Do global pollination by  $\mathbf{x}_i^{t+1} = \mathbf{x}_i^t + \gamma \cdot L(\lambda) \cdot (\mathbf{g}^* - \mathbf{x}_i^t)$ 
        else
            Draw  $\varepsilon$  from a uniform distribution in  $[0, 1]$ 
            Select randomly  $j$  and  $k$  among all flowers of the population
            Do local pollination by  $\mathbf{x}_i^{t+1} = \mathbf{x}_i^t + \varepsilon \cdot (\mathbf{x}_j^t - \mathbf{x}_k^t)$ 
        end if
        Evaluate objective function values of new solutions
        When better, update new solutions in the population
    end for
    Determine the best solution  $\mathbf{g}^*$  of the new population
end while

```

Figure 1. Pseudo-code of the FPA algorithm

3 Optimum design problem formulation

In this section, the structural design of a RC cantilever retaining wall is set as an optimization problem of the general form of Eq. (3), where $F(\mathbf{x})$ is the objective function and \mathbf{x} is the design solution vector that comprises of d independent design variables x_i ($i = 1$ to d). Furthermore, the solution should be subject to m number of constraints $g_j(\mathbf{x}) \leq 0$ ($j = 1$ to m).

$$\begin{aligned}
 &\text{Minimize:} && F(\mathbf{x}) \\
 &\text{Subject to:} && g_j(\mathbf{x}) \leq 0, \quad j = 1 \text{ to } m \\
 &\text{Where:} && \mathbf{x} = (x_1, x_2, \dots, x_d)
 \end{aligned} \tag{3}$$

Herein, six independent design variables x_i ($i = 1$ to 6) are used to describe the geometry of the concrete wall as shown in Fig. 2. The variables x_1 and x_3 are the stem thicknesses at the top and bottom respectively. The variables x_2 and x_4 represent the lengths of the footing toe and heel respectively. The variable x_5 is the footing thickness and the variable x_6 is the additional depth of the heel beam that this used to increase sliding resistance. The width t of the heel beam is treated as a fixed parameter with value t as it is not expected to influence significantly the

design of the wall. The wall height h is also considered as fixed parameter determined by the soil profile of the problem under investigation. Having established geometry, standard structural design of the wall is conducted assuming all other design parameters as fixed. The latter include soil and material properties, the surcharge loading q as well as the coefficients of active K_a and passive earth pressure K_p in addition to the coefficient of friction μ at the base of the wall.

The constraints of the optimization problem are set in accordance with the requirements of the RC retaining walls structural design as specified in Eurocode 7 (EC7) (CEN 2004). The design of these walls consists of three basic phases: 1) stability analysis; 2) bearing pressure analysis; 3) members design and detailing (Mosley *et al.* 2012).

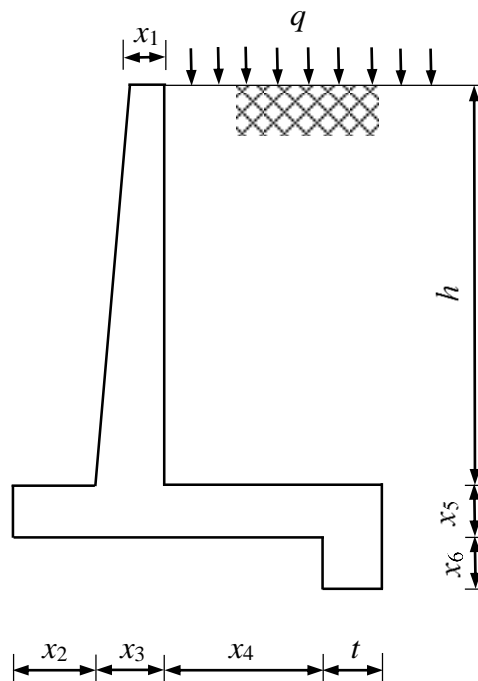


Figure 2. Design variables and parameters of the concrete cantilever retaining wall

The stability analysis phase consists of two checks. The overturning and the sliding stability checks. The former check is realised by comparing the design overturning moment about the bottom corner of the footing toe M_{Ed}^o with the overturning design moment resistance about the same point M_{Rd}^o as shown in Eq. (4). In the calculation of M_{Ed}^o and M_{Rd}^o , partial safety factors are used to the characteristic values of the loads depending on whether they are permanent or live loads and whether they have favourable or unfavourable effects on the design check. The values of the partial safety factors are taken by the UK National Annex of EC7. The active earth pressure and the surcharge lateral pressure are the loads with unfavourable effects and the weights of the wall and the soil resting on the wall are the loads with favourable effects.

$$\frac{M_{Ed}^o}{M_{Rd}^o} - 1 \leq 0 \quad (4)$$

In a similar manner, the sliding check is conducted by comparing the design sliding force H_{Ed}^S at the base of the footing with the design sliding resistance H_{Rd}^S as shown in Eq. (5). The resistance to sliding is provided by the friction at the base of the wall as well as the passive earth pressure over the depth of the heel beam.

$$\frac{H_{Ed}^S}{H_{Rd}^S} - 1 \leq 0 \quad (5)$$

In the second phase of the wall design procedure, the bearing stresses underneath the retaining walls are evaluated and the maximum values p_{max} are compared with the corresponding maximum allowable values p_{all} specified by the soil type. The bearing pressures are calculated as the combined effect of an equivalent overturning moment M about the centroid of the footing base and a concentric vertical load N following standard procedures.

$$\frac{p_{max}}{p_{all}} - 1 \leq 0 \quad (6)$$

Furthermore, to avoid uplift, the eccentricity $e = M / N$ should not be greater than $1/6^{\text{th}}$ (“middle third rule”) of the total footing length D (i.e. $D = x_2 + x_3 + x_4 + t$) as prescribed in Eq. (7).

$$\frac{6e}{D} - 1 \leq 0 \quad (7)$$

The last phase of the cantilever wall design procedure is the design of the bending reinforcement of the stem, toe and heel. Standard RC sections design procedures are applied herein. Moreover, different bending reinforcement is used in the top and bottom half of the stem of the wall to reduce costs but also maintain simplicity in construction. Furthermore, for construction simplicity, it is assumed that the heel and toe bending reinforcement extend along the full length of the top and the bottom sides of the footing of the wall respectively. In this design phase, the design constraints require that the longitudinal reinforcement ratio ρ_l should not exceed the allowable maximum steel reinforcement ratio ρ_{max} as prescribed in Eq. (8). It is also recalled that if ρ_l is smaller than the minimum allowable ratio ρ_{min} then the minimum

longitudinal reinforcement has to be placed. The volumetric ratios limits ρ_{max} and ρ_{min} are the same as the ones prescribed for RC beams in Eurocode 2 (EC2) (CEN 2000).

$$\frac{\rho_l}{\rho_{max}} - 1 \leq 0 \quad (8)$$

The objective function $F(\mathbf{x})$ is taken herein as the sum of the concrete C_c and reinforcing steel C_s material costs, the cost of formwork C_f and the cost of soil excavations C_e following Eq. (9), where m_i and p_i ($i = c, s, f, e$) are the material quantities and the corresponding unit prices respectively. All costs refer to one meter wall length. The material unit prices used in this study are given in Table 1 based on the Hellenic Ministry of Public Works (HMPW 2013). Furthermore, a penalty term is added to $F(\mathbf{x})$ to account for violations of the constraints of Eqs (4)-(8).

$$F(\mathbf{x}) = \sum_i C_i = \sum_i m_i \cdot p_i \quad (i = c, s, f, e) \quad (9)$$

Table 1. Material unit prices

Material	p_i	Unit
Concrete C30/37	116	m^3
Steel B500c	1.07	Kg
Falsework	15.7	m^2
Excavation works	7	m^3

4 Application case study

4.1 Introduction

In this section, a case study RC retaining wall is optimally designed using FPA. The design example is taken from the book of Mosley *et al.* (2012), where the design variables values used to determine wall geometry are given in Table 2. In this example, the following fixed problem parameters are used: concrete grade C30/37; reinforcing steel grade B500c; $q = 10 \text{ kN/m}^2$; $K_a = 0.33$; $K_p = 3.5$; $\mu = 0.45$; $h = 4500 \text{ mm}$; $t = 500 \text{ mm}$. Furthermore, the density of the granular material supported by the wall is $\rho_{soil} = 1700 \text{ kg/m}^3$. It is also assumed that the bearing capacity of the underlying soil is high enough and it does not affect the design. Using Eq. (9), the cost of the wall following the solution presented in Mosley *et al.* (2012) is calculated as €953.80/m.

In the same table, the design variables of the best design solution obtained by FPA are presented. It is worth noting that a value of $x_6 = 0$ mm is suggested by FPA, which essentially means that no heel beam is required to satisfy the sliding check of Eq. 5 and a uniform footing thickness is applied. This finding is meaningful from an engineering point of view since the sliding resistance coming from friction at the base of the wall is adequate to resist the sliding force demand. This optimal solution will be used as a reference in the following as it is the best solution derived after several FPA trials. The optimal cost of this design solution is €681.82/m which represents a 29% reduction with respect to the conventional design approach (Mosley *et al.* 2012).

Table 2. Design variables

Variable	Description	Mosley <i>et al.</i> (2012)	FPA optimal	Units
x_1	Stem thickness at top	300	251	mm
x_2	Length of footing toe	800	613	mm
x_3	Stem thickness at bottom	400	251	mm
x_4	Length of footing heel	2200	2494	mm
x_5	Footing thickness	400	276	mm
x_6	Additional depth of heel beam	600	0	mm

4.2 FPA parameters tuning

As discussed in the previous, this is the first study applying FPA to the structural design of RC retaining walls. Hence, it is important that the overall performance of FPA is investigated and its parameters are tuned to better address this optimization problem landscape. More particularly, the effects of n , p , λ and γ will be examined herein.

Table 3 presents the outcomes of ten different FPA runs after 2000 iterations with population size $n = 20$, $\lambda = 3/2$, $\gamma = 0.01$ and assuming different switch probability values p ranging between 0 and 1 by an increment of 0.1. In this table, the average, minimum and maximum costs obtained by the ten FPA trials are presented as well as their coefficient of variation. It is evident that, on average, the FPA yields very good predictions for most of the switch probability values. Nevertheless, the quality of the results decreases significantly for the extreme p values (i.e. $p = 0, 1$). This is the case because for the extreme p values FPA conducts only either global or local pollination and therefore it is not able to combine exploration and exploitation of the search space. Values of p between 0.1 and 0.9 give generally very good and

similar results. The quality of the results further improves for p values between 0.4 and 0.7. The best FPA performance is obtained by setting the switch probability $p = 0.5$ since this value exhibits both the best average cost and the minimum coefficient of variation.

Table 3. FPA outcomes for different switch probability values

p	Average Cost (€/m)	Minimum Cost (€/m)	Maximum Cost (€/m)	Coefficient of variation (%)
0	880.65	681.83	1158.17	8.87772
0.1	681.99	681.83	836.98	0.03162
0.2	685.41	681.83	716.47	1.59262
0.3	685.50	681.82	716.81	1.60494
0.4	681.83	681.82	681.86	0.00158
0.5	681.83	681.82	681.84	0.00093
0.6	681.83	681.82	681.89	0.00322
0.7	681.85	681.82	682.11	0.01320
0.8	685.88	681.83	711.56	1.34938
0.9	695.36	681.92	718.48	2.19466
1	836.98	738.50	1034.90	11.66593

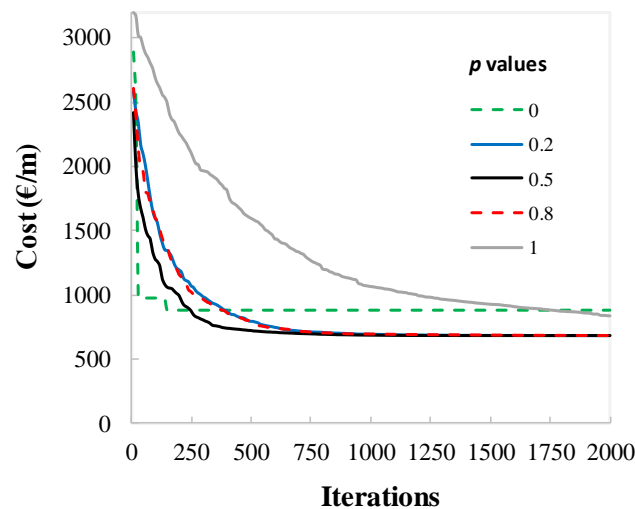


Figure 3. Iteration histories for different p values

Furthermore, Fig. 3 shows the average iterations histories derived by the FPA simulations with different p values. Not all probability values are presented for illustration reasons. It can be seen that the $p = 1$ value yields the slowest convergence. For $p = 0$, the initial convergence is rapid but then the algorithm is not able to improve its performance. For probability value $p = 0.5$, the best convergence response is achieved. In this case, the FPA algorithm requires approximately 500 iterations to reach convergence. Similar response is generally observed for

p values between 0.4 and 0.7. The solutions with $p = 0.2$ and 0.8 converge eventually to approximately the same solution as $p = 0.5$. However, they converge at a slower pace, which means that more computation effort is required to reach the optimum solution.

In addition to the switch probability value, the role of the population size is also examined herein. Table 4 presents the outcomes of ten different FPA runs for 2000 iterations with switch probability value $p = 0.5$, $\lambda = 3/2$, $\gamma = 0.01$ and three different population sizes: $n = 10, 20$ and 30. It is found that the population size has only a minor effect on the results. A population size of $n = 10$ has only marginally higher average cost than $n = 20$. For $n \geq 20$, the average cost remains practically constant.

Table 4. FPA outcomes for different population sizes

n	Average Cost (€/m)	Minimum Cost (€/m)	Maximum Cost (€/m)	Coefficient of variation (%)
10	681.91	681.82	682.71	0.04121
20	681.83	681.82	681.84	0.00093
30	681.82	681.82	681.82	1.75e-14

Furthermore, Fig. 4 shows the average iteration histories of the solutions with the different population sizes. It is seen that all solutions converge almost to the same solution. However, the $n = 10$ solution converges later than the larger population sizes. This partly counteracts the savings in reaching the optimum solution by reducing the population size. On the other hand, the population sizes $n = 20$ and 30 converge almost at the same pace. Hence, the use of $n = 30$ instead of $n = 20$ seems unnecessary as it increases the computational cost.

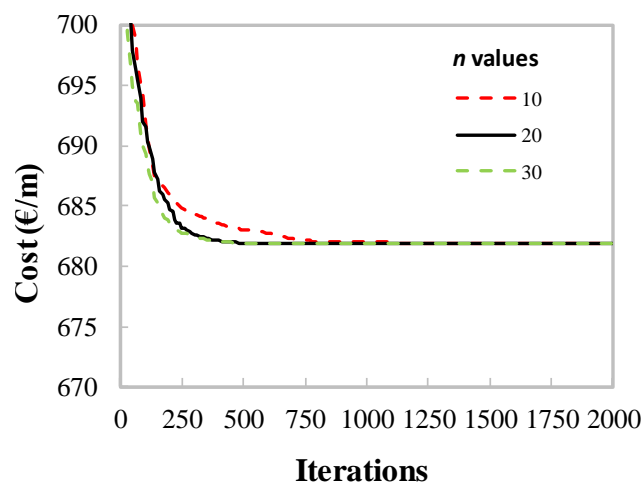


Figure 4. Iteration histories for different n values

Table 5 shows the outcomes of ten different FPA runs after 2000 iterations with population size $n = 20$, $\gamma = 0.01$, $p = 0.5$ and three different λ values ($\lambda = 1, 3/2$ and 2). It is clear that all λ values yield excellent results with $\lambda = 1$ leading to the minimum coefficient of variation. Moreover, Fig. 5 shows the average iterations histories derived by the FPA simulations with different λ values. It can be seen that the $\lambda = 3/2$ value provides the fastest convergence to the optimum value. Slightly worse convergence is achieved by $\lambda = 1$. The worst convergence performance is achieved by the $\lambda = 2$ value.

Table 5. FPA outcomes for different λ values

λ	Average Cost (€/m)	Minimum Cost (€/m)	Maximum Cost (€/m)	Coefficient of variation (%)
1	681.82	681.82	681.82	1.55e-05
3/2	681.83	681.82	681.84	9.30e-04
2	681.82	681.82	681.82	3.71e-05

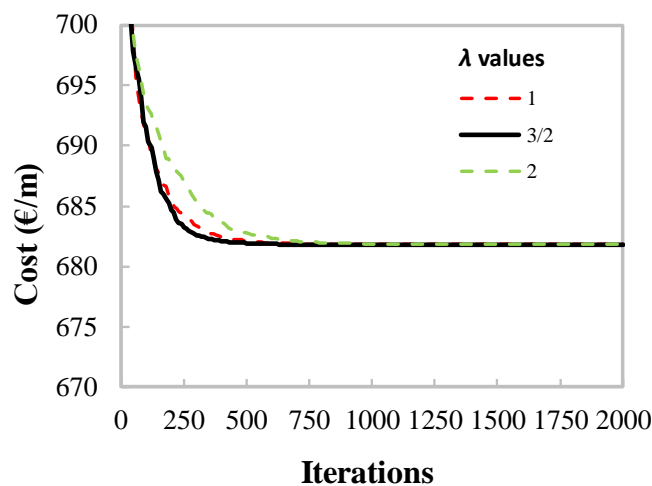


Figure 5. Iteration histories for different λ values

Table 6 presents the outcomes of ten different FPA runs after 2000 iterations with population size $n = 20$, $p = 0.5$, $\lambda = 3/2$ and six different γ values (i.e. $\gamma = 0.005, 0.01, 0.05, 0.1, 0.5$ and 1). It is evident that all γ values provide excellent results with very small and similar coefficients of variation. The $\gamma = 0.05$ value drives to the minimum coefficient of variation but again it is emphasized that the differences are rather insignificant. Furthermore, Fig. 6 illustrates the average iterations histories derived by the FPA simulations with the different γ values. It is found that convergence rate increases as the scaling factor to the step size γ increases from 0.005 to 0.5 . However, the opposite takes place when γ increases from 0.5 to 1 . This effectively

means that the $\gamma = 0.5$ value yields the best convergence performance for the problem under investigation.

Table 6. FPA outcomes for different γ values

γ	Average Cost (€/m)	Minimum Cost (€/m)	Maximum Cost (€/m)	Coefficient of variation (%)
0.005	681.82	681.82	681.82	0
0.010	681.83	681.82	681.84	9.30e-04
0.050	681.82	681.82	681.82	3.71e-05
0.100	681.82	681.82	681.82	8.84e-05
0.500	681.82	681.82	681.83	2.65e-04
1.000	681.83	681.82	681.87	2.14e-03

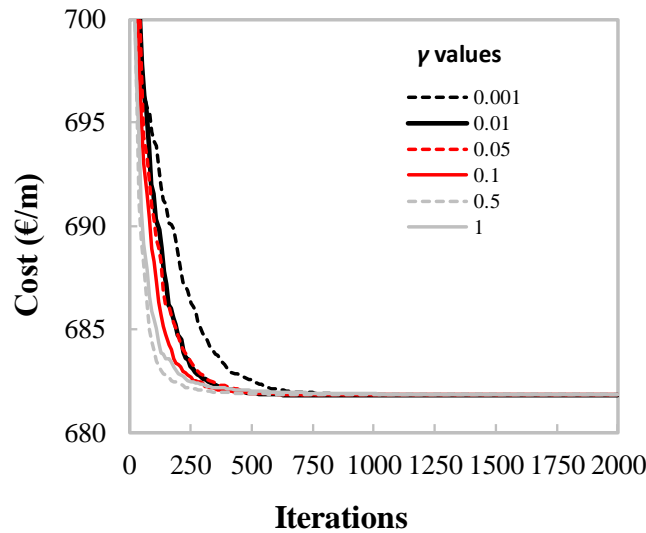


Figure 6. Iteration histories for different γ values

4.3 Comparison with PSO and GA

In this section, the FPA is compared with the PSO and GA algorithms in terms of computational performance. Similarly to FPA, a population size of 20 individuals and 2000 maximum iterations are used for the PSO and GA algorithms.

The standard PSO version is used herein. It is noted, however, that enhanced PSO versions have been developed to improve the computational performance of this algorithm (e.g. Yang *et al.* 2011, Wang *et al.* 2019a, Wang *et al.* 2019b). Furthermore, to identify the inertia coefficient that yields the best PSO performance for the problem under investigation, a parametric study is conducted herein. The statistics of the PSO results for the different inertia coefficients and ten independent runs are shown in Table 7. It is deduced that the best PSO

performance is obtained by setting its inertia coefficient equal to 1 and this is the value used in the rest of this study. With respect to GA, the version implemented in MATLAB R2017a (MathWorks 2017) is used. Default parameters values as suggested in MathWorks (2017) are applied. After ten runs, the average cost obtained by GA is €805.35/m, the minimum €751.34/m and the coefficient of variation is 4.95%.

The performances of PSO and GA are now compared with the performance of FPA for $n = 20$ and $p = 0.5$, $\gamma = 0.5$ and $\lambda = 3/2$ that yielded the best computational performance of FPA in the previous section. Comparing PSO with FPA, both algorithms determine almost the same minimum cost. However, the average cost calculated by PSO is considerably (2.2%) higher than the one of FPA. The coefficient of variation is also higher in the case of PSO. It is noted that these differences may look insignificant per wall meter but they can become important when walls extend along several kilometres in road construction. Comparing GA with FPA, it is clear that FPA performs significantly better than GA both in terms of minimum costs and coefficients of variation.

Table 7. PSO outcomes for different switch probability values

<i>Inertia</i> <i>Coefficient</i>	Average Cost (€/m)	Minimum Cost (€/m)	Maximum Cost (€/m)	Coefficient of variation (%)
0	711.43	681.86	724.39	2.21060
0.1	724.74	716.28	775.71	2.50547
0.2	707.63	681.83	722.78	2.31792
0.3	711.87	681.83	729.77	2.27078
0.4	711.95	681.83	725.82	2.27078
0.5	726.89	681.83	767.94	4.31511
0.6	704.08	681.83	722.69	2.72863
0.7	712.54	681.84	724.63	2.29491
0.8	716.28	681.83	730.45	1.79413
0.9	704.73	681.83	766.67	4.00127
1	696.66	681.83	721.18	2.75076

Furthermore, Fig. 7 presents a comparison of the convergence performance of the FPA and the GA and PSO algorithms. Figure 7a compares the average cost histories and Fig. 7b the normalized errors in logarithmic scale of the average cost histories (i.e. $\text{error} = (\text{cost} - 681.82) / 681.82$) of all three algorithms with respect to the minimum cost achieved (i.e. €681.82/m of the reference FPA solution). It can be seen that the FPA algorithm provides better performance from the early iteration steps and it drives to significantly more accurate results at the end of the analyses. It is also clear that FPA approaches the minimum cost almost exponentially with

the number of iterations. On the other hand, PSO reduces the error in the first iteration steps but is not able to yield more accurate predictions after a specific iteration step (approx. 220). This can be attributed to the relatively poor exploration capacity of the PSO algorithm in the later stage of iterations that allows it to be trapped in local optimal solutions (Li *et al.* 2015). The error of GA remains significant throughout the iterations history.

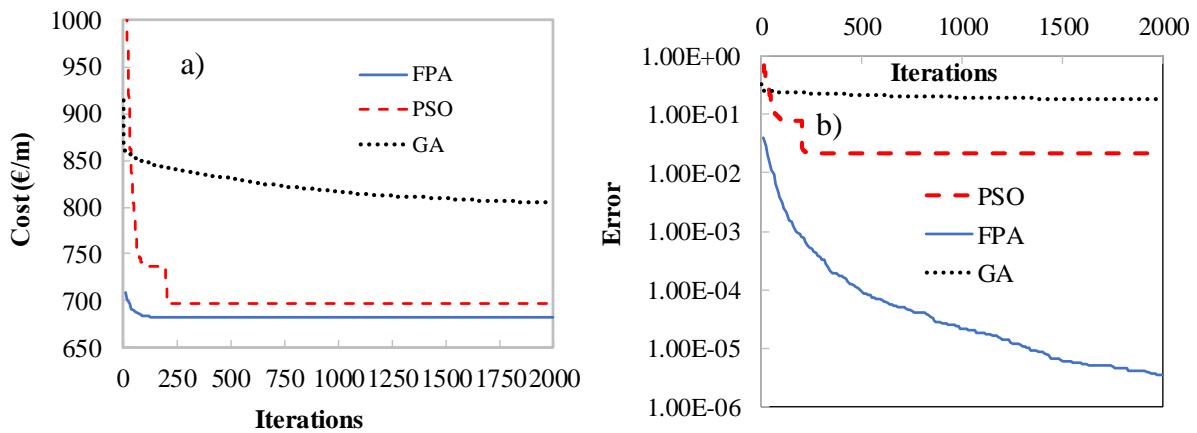


Figure 7. Comparison of FPA with PSO and GA performances; a) average cost histories; b) average normalized error histories

4.4 Parametric optimum designs and further comparisons with PSO and GA

In this section, the costs of optimum designs of the RC retaining wall as a function of the wall height h and the surcharge loading q are presented. All costs are derived by using FPA with $p = 0.5$, $n = 20$, $\gamma = 0.5$ and $\lambda = 3/2$ and 2000 maximum iterations. The FPA predictions are also compared with the respective PSO and GA predictions for the respective h and q values. This parametric study is important as it can affect decision making in the early phases of the wall design. Both optimum cost variations are presented in Fig. 8. Average costs are presented therein based on the results of ten independent algorithm runs for each h and q value.

In Fig. 8a, optimum costs are presented for wall heights ranging from 2 to 14 meters with a step of 0.5 m. It can be seen that cost increases rapidly and nonlinearly with the height of the wall. Increasing the height of the wall from 4m to 14m can increase the cost almost by ten times. Similar findings are reported in Yepes *et al.* (2008). Furthermore, Fig. 8b shows the variation of optimum wall costs with the magnitude of surcharge loading q . Results are presented for q values ranging from 0 to 20 kN/m² with a step of 1 kN/m². It is evident that the cost of the walls increases almost linearly with the magnitude of the surcharge loading.

However, the rate of increase is rather slow. An increase of q from zero to 20 kN/m^2 drives only to approximately 25% increase in the wall costs.

In all comparisons of FPA with PSO and GA algorithms in Fig. 8, FPA provides lesser or equal costs to the PSO and GA algorithms. In Fig. 8a, it can be concluded that the differences in costs achieved by the three algorithms become more significant for large walls heights, where high costs are generally involved. Furthermore, in Fig. 8b, it is shown that the FPA predicts a clear linear trend of the walls cost and surcharge loading. On the other hand, the PSO and GA algorithms fail to yield a clear trend of wall costs with surcharge loading. It is worth noting that in some cases PSO and GA predict a decrease of minimum cost with an increase of the surcharge loading, which is counter-intuitive.

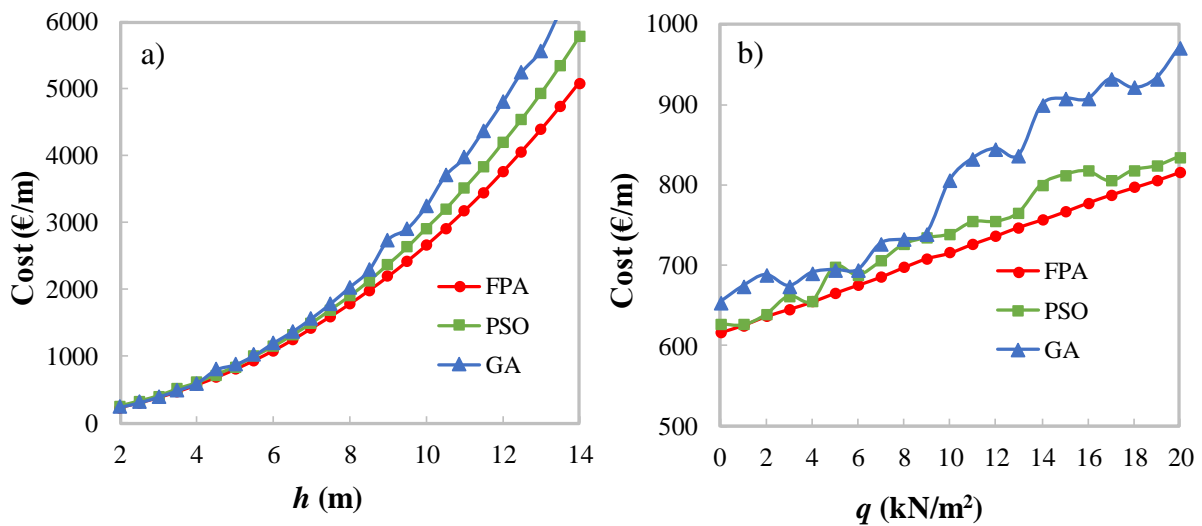


Figure 8. Average optimum costs achieved by FPA and PSO as a function of a) h ; b) q

5 Conclusions

FPA is a novel optimization algorithm mimicking the evolution process of flowering species. Following its development, it has been applied to various optimization problems in different scientific fields. Despite the fact that several studies exist on the optimization of RC retaining walls, none of these studies has employed FPA to obtain the optimum solutions.

To fill this gap, the present study applies FPA to the optimum structural design of an RC cantilever retaining wall case study with six independent design variables. It is found that FPA reduces significantly the cost of the wall with respect to conventional design approaches. Furthermore, parametric studies are conducted to identify the FPA parameters that provide the best performance of this algorithm on the optimization problem of the present study. It is found

that switch probability values p ranging between 0.4 and 0.7 yield the optimum performance in terms of both minimum costs and convergence performance. Switch probability values of 0.2 and 0.8 still drive to optimal costs but they converge at a slower pace. On the other hand, the extreme switch probability values $p = 0$ and 1 are not typically able to track the global optimal solutions. Moreover, the effect of the population size is investigated. It is found that the performance of FPA is not significantly affected by the population size for the problem under investigation. More particularly, a population size of 20 individuals offers a good balance between performance and computational effort. Populations with more than 20 individuals do not seem to improve the final results as well as the rate of convergence. Populations with less than 20 individuals reach ultimately the same optimum costs but they require more iterations to converge.

Furthermore, the effect of constant λ of the Lévy flight step size $L(\lambda)$ is also examined. It is found that solutions with λ values between 1 and 2 converge eventually to similar minimum costs. However, the rate of convergence is maximised if λ is set equal to $3/2$ as also recommended by Yang (2012). Finally, the influence of the Lévy flight step size scale factor γ on the performance of FPA is investigated. It is concluded that γ does not affect considerably the ultimate optimum costs achieved by FPA. However, it strongly affects the rate of convergence of the algorithm. For the design of RC retaining walls, it is found that $\gamma = 0.5$ offers the best convergence rate of the FPA algorithm.

The efficiency of FPA in solving the optimization problem of this study is compared with the one of the PSO and GA algorithms for a great number of different wall configurations. It is generally found that FPA outperforms both PSO and GA yielding lesser costs and with smaller variability.

Finally, a parametric study is conducted to investigate the effects of the wall height and surcharge loading on the optimum costs of RC cantilever retaining walls. It is concluded that the optimum costs increase rapidly and nonlinearly with the wall height. On the other hand, they increase almost linearly but rather smoothly with the surcharge loading.

Conflict of interest

On behalf of all authors, the corresponding author states that there is no conflict of interest.

Replication of results

The Flower Pollination Algorithm (FPA) used in this study is readily available in the MATLAB file exchange system. Furthermore, the conventional design of the reinforced concrete retaining wall case study examined herein is presented in Mosley *et al.* (2012). It is noted that the FPA algorithm is based on stochastic processes. Hence, exact replication of the results presented in this study is not possible.

References

- Aydogdu I (2017). Cost optimization of reinforced concrete cantilever retaining walls under seismic loading using a biogeography-based optimization algorithm with Levy flights. *Engineering Optimization* 49(3): 381-400.
- Alyasserri ZAA, Khader AT, Al-Betar MA, Awadallah MA, Yang XS (2018). Variants of the flower pollination algorithm: A review. *Studies in Computational Intelligence*, 91-118.
- Babu S, Basha MB (2008). Optimum design of cantilever retaining walls using target reliability approach. *ASCE International Journal of Geomechanics* 8(4): 240-252.
- Bekdas G, Nigdeli SM, Yang XS (2015). Sizing optimization of truss structures using flower pollination algorithm. *Applied Soft Computing* 37: 322-331.
- CEN (2000). Eurocode 2: Design of concrete structures. Part 1-1: General rules and rules for buildings. Brussels: European Standard EN 1992-1-1.
- CEN (2004). Eurocode 7: Geotechnical design. Brussels: European Standard EN 1997.
- Ceranic B, Fryer C, Baines RW (2001). An application of simulation annealing to the optimum design of reinforced concrete retaining structures. *Computers and Structures* 79: 1569-1581.
- Gandomi AH, Yang XS, Alavi AH (2013). Cuckoo search algorithm: a metaheuristic approach to solve structural optimization problems. *Engineering Computation* 29: 17-35.
- Gandomi AH, Kashani AR, Roke DA, Mousavi M (2017). Optimization of retaining wall design using evolutionary algorithms. *Journal of Structural and Multidisciplinary Optimization* 55: 809-825.
- Ghazavi M, Bonab SB (2011). Learning from ant society in optimizing concrete retaining walls. *Journal of Technology and Education* 5(3): 205-212.
- Glover BJ (2007). *Understanding flowers and flowering: An integrated approach*. Oxford University Press, UK.
- Holland JH (1975). *Adaptation in natural and artificial systems. An introductory analysis with application to biology, control and artificial intelligence*. University of Michigan, Ann Arbor, MI.
- HMPW (2013). *Readjustment and completion of invoices of public works*, Hellenic Ministry of Public Works, Athens, Greece.
- Kaveh A, Abadi ASM (2010). Harmony search based algorithm for the optimum cost design of reinforced concrete cantilever retaining walls. *International Journal of Civil Engineering* 9(1): 1-8.
- Kaveh A, Abadi ASM (2014). Optimal design of cantilever retaining walls using ray optimization method. *IJST Transactions of Civil Engineering* 38(1): 261-274.
- Khajehzadeh M, Taha MR, El-Shafie A, Eslami M (2010). Economic design of retaining wall using particle swarm optimization with passive congregation. *Australian Journal of Basic and Applied Sciences* 4(11): 5500-5507.
- Khajehzadeh M, Taha MR, Eslami M (2014). Multi-objective optimisation of retaining walls using hybrid adaptive gravitational search algorithm. *Civil Engineering and Environmental Systems* 31(3): 229-242.
- Kennedy J (2011). Particle swarm optimization. *Encyclopedia of Machine Learning*, 760-766, Springer.
- Li Z, Wang W, Yan Y, Li Z (2015). PS-ABC: A hybrid algorithm based on particle swarm and artificial bee colony for high-dimensional optimization problems. *Expert Systems with Applications*, 42: 8881-8895.
- MathWorks, MATLAB R2017a – Global Optimization Toolbox, Natick, MA, USA: The MathWorks Inc, 2000.

- Mergos (2017). Optimum seismic design of reinforced concrete frames according to Eurocode 8 and *fib* Model Code 2010. *Earthquake Engineering and Structural Dynamics* 46: 1181-1201.
- Mergos (2018a). Seismic design of reinforced concrete frames for minimum embodied CO₂ emissions. *Energy and Buildings* 162: 177-186.
- Mergos (2018b). Contribution to sustainable seismic design of reinforced concrete members through embodied CO₂ emissions optimization. *Structural Concrete* 19: 454-462.
- Mergos (2019). Efficient optimum seismic design of reinforced concrete frames with nonlinear structural analysis procedures. *Structural and Multidisciplinary Optimization* 58: 2565-2581.
- Mosley B, Bungey J, Hulse R (2012). Reinforced concrete design to Eurocode 2. 7th Edition, Palgrave McMillan, UK
- Nigdeli SM, Bekdaş G, Yang XS (2016). Application of the flower pollination algorithm in structural engineering. In: *Metaheuristics and Optimization in Civil Engineering*, 28-42, Springer.
- Nigdeli SM, Bekdaş G, Yang XS (2017). Optimum tuning of mass dampers by using a hybrid method using harmony search and flower pollination algorithm. In: *International Conference on Harmony Search Algorithm*, 222–231. Springer
- Papazafeiropoulos G, Plevris V, Papadrakakis M (2013). Optimum design of cantilever walls retaining linear elastic backfill by use of genetic algorithm. *Computational Methods in Structural Dynamics and Earthquake Engineering (COMPDYN) Conference*, Kos, Greece.
- Pavlyukevich I (2007). Lévy flights, non-local search and simulated annealing. *Journal of Computational Physics* 226: 1830-1844.
- Pei Y, Xia Y (2012). Design of reinforced cantilever retaining walls using heuristic optimization algorithms. *Procedia Earth and Planetary Science* 5: 32-36.
- Saribas A, Erbatur F (1996). Optimization and sensitivity of retaining structures. *ASCE Journal of Geotechnical Engineering* 122(8): 649-656.
- Sheikholeslami R, Khalili BG, Sadollah A, Kim JH (2016). Optimization of reinforced concrete retaining walls via hybrid firefly algorithm with upper bound strategy. *KSCE Journal of Civil Engineering* 20(6): 2428-2438.
- Rahbari P, Ravichandran N, Juang HC (2017). Seismic geotechnical robust design of cantilever retaining wall using response surface approach. *Journal of Geoengineering* 12(4): 147-155.
- Yang XS (2008). *Nature-inspired metaheuristic algorithms*. Luniver Press, UK.
- Yang XS (2010). Firefly algorithm, stochastic test functions and design optimization. *International Journal of Bio-inspired Computation* 2: 78-84.
- Yang XS, Deb S, Fong S (2011). Accelerated particle swarm optimization and support vector machine for business optimization and applications. In: *Networked digital technologies*. Berlin, Heidelberg: Springer-Verlag: 53–66.
- Yang XS (2012). Flower pollination algorithm for global optimization. *Unconventional Computation and Natural Computation* 7445: 240-249.
- Yepes V, Gonzalez-Vidosa F, Alcalá J, Villalba P (2008). A parametric study of optimum earth-retaining walls by simulated annealing. *Engineering Structures* 30: 821-830.
- Yepes V, Alcalá J, Perea C, Gonzalez-Vidosa F (2012). CO₂-Optimization design of reinforced concrete retaining walls based on a VNS-Threshold Acceptance Strategy. *Journal of Computing in Civil Engineering* 26(3): 378-386.
- Wang C, Yu T, Curiel-Sosa JL, Xie N, Bui TQ (2019a). Adaptive chaotic particle swarm algorithm for isogeometric multi-objective size optimization of FG plates. *Journal of Structural and Multidisciplinary Optimization* 60: 757-778.
- Wang C, Yu T, Shao G, Nguyen TT, Bui TQ (2019b). Shape optimization of structures with cutouts by an efficient approach based on XIGA and chaotic particle swarm optimization.